J Intell Robot Syst (2014) 74:333–346
DOI 10.1007/s10846-013-9899-2

Cooperative Control of Multiple UAVs for Moving Source Seeking

Senqiang Zhu · Danwei Wang · Chang Boon Low

Received: 31 August 2013 / Accepted: 11 September 2013 / Published online: 12 October 2013

Abstract Advances in multi-agent technologies and UAV technologies make it possible to take advantage of cooperation of multiple UAVs for source seeking. This paper focuses on moving source seeking using multiple UAVs with input constraints. Firstly, a least-squares method is introduced to estimate the gradient of the scalar field at the leader UAV location based on the measurements of all UAVs. Since the moving source velocity is unknown, an adaptive estimator is designed to obtain the velocity. Based on the estimated gradient and source velocity, a guidance law and a sliding mode based heading rate controller are proposed for the leader UAV to achieve level tracking. Heading rate controller for each follower UAV is also developed to achieve circular formation around the leader UAV. Furthermore, the gradient estimation error is analyzed and its influence on moving source velocity estimation and level tracking accuracy is explored as well. Finally, simulation results are provided to verify the proposed approach.

Keywords UAV · Source seeking · Formation control · Adaptive estimation

S. Zhu (✉) · D. Wang
EXQUISITUS, Centre for E-City, School of Electrical and Electronic Engineering, Nanyang Technological University, 639798 Singapore, Singapore
e-mail: zhusenqiang@gmail.com

D. Wang
e-mail: edwwang@ntu.edu.sg

C. B. Low
DSO National Laboratories, INFO Division, Manned-Unmanned Programme, 27 Medical Drive, 117510 Singapore, Singapore
e-mail: lchangbo@dso.org.sg

1 Introduction

The increasing military and civilian applications have greatly spurred the UAV research development in the past decade. Recently, the problem of source seeking has received much attention [1–6]. With the development of multi-agent technologies and UAV technologies, cooperation of multiple UAVs becomes one choice for source seeking. In the real world, there are various sources which can generate vector fields or scalar fields. Scalar fields may represent the temperature distribution throughout space, the strength of an acoustic signal, the concentration of a chemical agent, etc. In each scalar field, there may exist one or more sources which could be pointwise, area, or volume sources. Scalar field source seeking is to find the

source using one or more agents based on the measured data. Many different approaches have been proposed to solve this problem in the literature. These works can mainly be classified into two categories: single-agent source seeking and multi-agent source seeking.

For single-agent source seeking, if the gradient of the scalar field can be directly measured, then the source localization or seeking can be achieved by adopting a simple gradient climbing strategy. However, most agents can only measure the scalar field value instead of the gradient. In order to estimate the scalar field gradient, one commonly used method is to maneuver the robot with sinusoidal inputs [1, 2]. An angular velocity controller for a nonholonomic agent is proposed to achieve source seeking in [1], while the forward speed is tuned to achieve source seeking with constant angular velocity in [2]. By using a sliding mode based method, source seeking can also be achieved without gradient estimation in [3]. The proposed sliding mode based turning rate controller can drive the robot to the desired vicinity of the field maximizer in a finite time and afterwards the robot remains in this region. However, since the change rate of the field value is required in [3], the measurement noise may result in a significant error in the computation. In [7], a stochastic source seeking approach is proposed for the nonholonomic mobile robot to converge to the unknown source. Firstly, a stochastic trajectory is generated by extending simultaneous perturbation stochastic approximation technique, and then a simple source seeking controller is designed to follow this trajectory so that switching source seeking is achieved.

Cooperation of multiple robots for source seeking has several advantages over single robot, such as faster convergence, higher precision and more robust performance. There also has been a large body of research work in this area in the literature. In [4], mobile sensor networks are used to achieve gradient climbing in a sensed, distributed environment. The gradient climbing problem is decoupled into two tasks: formation stabilization and gradient climbing so that each task can be dealed with independently. In [8], a provably convergent cooperative Kalman filter is designed to estimate the gradient at the center of the formation. A geometric approach is adopted to design formation controllers, where the formation shape and orientation dynamics can be decoupled from the dynamics of the formation center based on the Jacobi transformation. However, the proposed control strategies in the above two papers are based on double integrator dynamics and therefore can not be directly applied to UAV control due to the physical constraints of the fixed wing UAV, such as nonholonomic property. A nonlinear filter is proposed in [9] for target tracking with range measurement only. Based on the measured range, the proposed nonlinear filter is used to estimate the position, velocity and acceleration of the target. However, this approach is not applicable to the problem of unknown scalar field source seeking since the structure of the field distribution is unknown. In [10], a gradient climbing problem to steer a group of vehicles to the extremum of an unknown scalar field distribution is studied. In this paper, the leader is first used to estimate the gradient by dithering its position, and after that the leader is controlled to achieve gradient climbing. The followers are controlled to follow the leader by using passivity based coordination rules. It is worth noting that the gradient is estimated by the leader only in this paper. In [11], the problem of multiagent deployment over a source is explored. Based on the heat partial differential equation and extremum seeking, a source seeking control algorithm is designed to deploy the group of agents around the source. Recently, communication constraints are taken into account for source seeking by several researchers. In [12], distributed source seeking is studied subject to all-to all and limited communication. Based on the gradient estimated by the group of robots, a cooperative controller is proposed to achieve source seeking, and furthermore, the theoretical upper bound on the tracking error is provided as well. In [13], collaborative estimation of gradient by a formation of AUVs under communication constraints is discussed. Under the assumption that the formation is fixed, the proposed consensus approach can achieve exact gradient estimation.

In [14], a circular formation of UAVs are used to achieve source seeking. In order to approximate the gradient direction, the UAVs are also required to be evenly separated on the circle. Variable airspeed and heading rate controllers are designed to attain such formation. However, it is difficult to guarantee that the agents are evenly distributed on the circular orbit if the formation center is time varying. Most of the above works assume that the sources or targets are stationary. In practice, there also exist many moving scalar field sources, such as acoustic signal on a moving vehicle.

UAV flight control has also been widely studied in the literature [15–24]. In [15, 16], Lyapunov guidance vector field approaches are used to guide UAVs to fly around a target in a circular formation. In [17], the problem of ground target tracking using single UAV with input constraints is investigated, where an adaptive observer is developed to estimate the unknown constant wind. Adversarial target tracking control is studied in [18], where the UAV must avoid exposure to the target or minimize the exposure time. Collective motion of multiple Newtonian particles in time invariant flowfield is studied in [19], where heading rate controller is designed for each agent to achieve circular formation. Later, following the paper [19], collective motion of multiple Newtonian particles in time varying flowfield is studied in [20, 21].

In our previous work [25], stationary source seeking is explored. As an extension, this paper focuses on the problem of unknown moving scalar field source seeking using multiple UAVs. The cooperative control strategy design is challenging due to the nonholonomic property of the fixed wing UAV. Meanwhile, due to the physical constraints of the fixed wing UAV, the UAV can not remain on top of the source. One choice for the UAV is to fly along a circular orbit around the source. Therefore, level tracking strategy is adopted so that UAVs can be located in the vicinity of the source. In order to fly the UAVs as a group, leader-follower formation strategy is utilized for multi-UAV cooperation. Firstly, a least-squares method is introduced to estimate the gradient of the scalar field at the leader UAV location based on the measurements of all UAVs. Since the moving source velocity is unknown, an adaptive estimator is designed to obtain the velocity. Based on the estimated gradient and velocity, a guidance law for the leader UAV is proposed. In order for the leader to follow the desired heading angle, a sliding mode based heading rate controller is designed. Heading rate controller for each follower UAV is also developed to achieve circular formation around the leader UAV. Furthermore, the gradient estimation error is analyzed and its influence on moving source velocity estimation and level tracking accuracy is explored as well.

2 Problem Statement

The problem of moving source seeking using multiple UAVs is described in this section. A commonly used UAV model with control input constraints is first introduced. Then, the unknown moving scalar field distribution is provided and the proposed problem in this paper is stated in detail.

2.1 UAV Model

The kinematic model of a fixed wing UAV under the assumption that the altitude is held constant is given by the following equations

$$\begin{aligned} \dot{x}_i &= v_i \cos\psi_i \\ \dot{y}_i &= v_i \sin\psi_i \\ \dot{\psi}_i &= w_i, \end{aligned} \tag{1}$$

where $col(x_i, y_i) \in \mathbf{R}^2$ is the two-dimensional position of the ith fixed wing UAV, $\psi_i \in [-\pi, \pi)$ is the UAV heading angle, v_i, w_i are the two control input signals which are commanded airspeed and heading rate respectively. In this paper, the airspeed v_i for each UAV is assumed to be constant, and however, different UAVs may have different airspeeds.

Due to the stall condition, the thrust limitation and roll angle limitation of the fixed wing UAV,

the following input constraints should be enforced on the UAV

$$0 < v_{\min} \le v_i \le v_{\max};\ |w_i| \le \omega_{\max}. \tag{2}$$

2.2 Source Seeking Problem

In order to illustrate the problem formulation clearly, firstly the unknown scalar field source properties need to be defined and described. It is assumed that there is a unique source in the scalar field and the location of the source is $\vec{r}_s = col(x_s, y_s)$. We also make the following assumptions for the source.

Assumption 1 The scalar field $f(\vec{r}) = f(||\vec{r}-\vec{r}_s||) : \mathbf{R}^2 \to \mathbf{R}$ is a concave function with respect to $\vec{r}$ and reaches its maximum at $\vec{r} = \vec{r}_s$ [12], where $\vec{r} = col(x, y)$ is the two-dimensional position of the UAV.

Assumption 2 The source is moving with a constant velocity $\dot{\vec{r}}_s = \vec{v}_s = col(v_{sx}, v_{sy})$ and $||\vec{v}_s|| < v_l$. The position and velocity of the source are unknown. UAVs can only measure the magnitude of the scalar field.

Assumption 3 The hessian matrix H of the scalar field satisfies the following condition: $-\delta_1 \le \lambda(H) \le -\delta_2$, where $\lambda(\cdot)$ represents the eigen value of the matrix and δ_1 and δ_2 are positive constants.

Remark 1 It is noted from Assumption 1 that, the scalar field value $f(\vec{r})$ only depends on the distance from the UAV current location to the source. For instance, $f(\vec{r}) = f_{\max}[1 - \tanh(\alpha||\vec{r} - \vec{r}_s||^{\beta})]$, $\alpha > 0$, $\beta > 0$. Since sources may be far away from the seeking agents like UAVs, it is reasonable to assume that the position and velocity of the source are unknown. In Assumption 2, v_l is a constant related to the UAV airspeed which will be determined in the sequel. The introduction of this constant makes it possible for UAVs to achieve source seeking. Assumption 3 implies that curvature of the scalar field is bounded.

Based on the above source definition and assumptions, now it is ready to analyze the source seeking problem. First of all, a cooperative strategy needs to be determined for multiple-UAV control mission. There are mainly three formation strategies: leader-follower, behavior-based, and virtual-structure. Since the gradient of the scalar field needs to be estimated based on the measurement data from multiple UAVs, leader-follower formation could be adopted where the leader UAV is used to process the gradient estimation. It is assumed that each follower UAV can get the position and velocity information of the leader UAV, and the leader UAV can get the positions and the scalar field values from all follower UAVs. With the Assumption 2, the constant source velocity is unknown, thus, source velocity estimation is needed in order to achieve accurate source seeking. As it is well known, the fixed-wing UAV can not stop on top of the source due to its physical constraints if the source velocity is lower. In addition, if the source is a hazardous source, the UAV must avoid to be too close to the source. Therefore, level tracking is carried out in this paper for source seeking. Level tracking implies that the UAV will fly along a trajectory around the source on which the scalar field has the same value. Based on the level tracking, the formation of UAVs can remain in the vicinity of the source. Now, it is ready to state the proposed problem.

Problem The objective of this paper is to design algorithms to estimate the gradient and source velocity under the Assumptions 1, 2 and 3, and based on these estimates, to develop controllers for UAVs so that level tracking around the source can be achieved. Furthermore, gradient estimation error and its influence on source velocity estimation error and level tracking accuracy also need to be studied.

3 Gradient and Moving Source Velocity Estimation

In this section, the scalar field gradient and moving source velocity are estimated. Firstly, a least-squares method is introduced to estimate the scalar field gradient. Secondly, the estimation error of the gradient is analyzed. Thirdly, moving

source velocity is estimated by using an adaptive observer. Lastly, the velocity estimation error is investigated in terms of the gradient error.

3.1 Gradient Estimate

As discussed in the previous section, the position of the source is unknown and only the scalar field value can be measured by each UAV. Unlike the approach for gradient estimate in [10], the proposed approach in this section requires the cooperation of all UAVs, including the leader and all followers.

Here, $\vec{r}_1 = col(x_1, y_1)$ denotes the leader position, $\vec{r}_i = col(x_i, y_i)$, $i = 2, 3, \cdots n,\ n \geq 3$, denotes the ith follower position, and $f_i, i = 1, 2, 3, \cdots, n$, denotes the scalar field value measured by the ith UAV. If there are n UAVs ($n \geq 3$), it is easy to ensure that the locations of UAVs are non-collinear. By using Taylor series expansion around the leader location, the first order approximation of the scalar field at the ith follower location is as follows:

$$f_i \approx f_1 + \frac{\partial f}{\partial x}|_{x=x_1}(x_i - x_1) + \frac{\partial f}{\partial y}|_{y=y_1}(y_i - y_1). \quad (3)$$

where $\nabla f = col(\frac{\partial f}{\partial x}|_{x=x_1}, \frac{\partial f}{\partial y}|_{y=y_1})$ is the scalar field gradient at the leader location. For simplicity, $(\frac{\partial f}{\partial x_1}, \frac{\partial f}{\partial y_1})$ will be used instead of $(\frac{\partial f}{\partial x}|_{x=x_1}, \frac{\partial f}{\partial y}|_{y=y_1})$, and $\vec{r}_{ij} = \vec{r}_i - \vec{r}_j, i = 1, 2, 3, \cdots, j = 1, 2, 3, \cdots$.

Then, stacking the approximations of the scalar field at all follower locations leads to the following equations:

$$\begin{bmatrix} f_2 - f_1 \\ f_3 - f_1 \\ \vdots \\ f_n - f_1 \end{bmatrix} \approx \begin{bmatrix} x_2 - x_1 & y_2 - y_1 \\ x_3 - x_1 & y_3 - y_1 \\ \vdots & \vdots \\ x_n - x_1 & y_n - y_1 \end{bmatrix} \bullet \begin{bmatrix} \frac{\partial f}{\partial x_1} \\ \frac{\partial f}{\partial y_1} \end{bmatrix}. \quad (4)$$

For the sake of simplicity, the notation P is introduced to denote the following matrix:

$$P = \begin{bmatrix} x_2 - x_1 & y_2 - y_1 \\ x_3 - x_1 & y_3 - y_1 \\ \vdots & \vdots \\ x_n - x_1 & y_n - y_1 \end{bmatrix}. \quad (5)$$

In order to estimate the gradient $(\frac{\partial f}{\partial x_1}, \frac{\partial f}{\partial y_1})$, a least-squares formula is used such that

$$\begin{bmatrix} G_x \\ G_y \end{bmatrix} = (P^T P)^{-1} P^T \begin{bmatrix} f_2 - f_1 \\ f_3 - f_1 \\ \vdots \\ f_n - f_1 \end{bmatrix}, \quad (6)$$

where $\vec{G} = col(G_x, G_y)$ is the estimated gradient at the leader location.

Since there exist noises in the measurement data and the first order approximation of the scalar field ignores the second and higher order terms, there may exist errors in the gradient estimation. In this section, the influence of the second order term of the Taylor series expansion on the gradient estimation error is analyzed. The following second order approximation of the scalar field is taken into account [4]:

$$f_i \approx f_1 + \nabla f \cdot \vec{r}_{i1} + \frac{1}{2}\vec{r}_{i1}^T H_1 \vec{r}_{i1}, \quad (7)$$

where, H_1 is the hessian matrix at the leader location. Then, it can be obtained that:

$$\nabla f = (P^T P)^{-1} P^T \begin{bmatrix} f_2 - f_1 \\ f_3 - f_1 \\ \vdots \\ f_n - f_1 \end{bmatrix} - \frac{1}{2}(P^T P)^{-1} P^T \begin{bmatrix} \vec{r}_{21}^T H_1 \vec{r}_{21} \\ \vec{r}_{31}^T H_1 \vec{r}_{31} \\ \vdots \\ \vec{r}_{n1}^T H_1 \vec{r}_{n1} \end{bmatrix}. \quad (8)$$

Subtracting Eq. 8 from Eq. 6 leads to the following result:

$$\Delta\vec{G} = \vec{G} - \nabla f = \frac{1}{2}(P^T P)^{-1} P^T \begin{bmatrix} \vec{r}_{21}^T H_1 \vec{r}_{21} \\ \vdots \\ \vec{r}_{i1}^T H_1 \vec{r}_{i1} \\ \vdots \\ \vec{r}_{n1}^T H_1 \vec{r}_{n1} \end{bmatrix}, \quad (9)$$

where $\Delta\vec{G} = col(\Delta G_x, \Delta G_y)$ is the gradient estimation error.

It can be observed from Eq. 9 that the gradient estimation error depends on the relative

positions between UAVs and the hessian matrix of the scalar field at the leader location. Thus, if the UAV formation is well designed, the gradient estimation error can be reduced. In this paper, circular formation is used where the leader UAV is located at the center of the formation and all follower UAVs fly along the circle around the leader as depicted in Fig. 1. In this circular formation, the distances between the leader UAV and follower UAVs are constant and could be short enough for communication. If the circular formation is assumed to be well maintained, it can be obtained that

$$\vec{r}_i = \vec{r}_1 + r_c(\cos\theta_i, \sin\theta_i)^T, , i = 2, 3, \cdots n, \tag{10}$$

where, r_c is the radius of the circular formation, θ_i is the clock angle of the ith follower UAV with respect to the leader. Substituting Eq. 10 into $(P^T P)^{-1}$ leads to that

$$\begin{aligned}(P^T P)^{-1} &= \frac{1}{r_c^2}\left(\sum_{i=2}^{n}\begin{bmatrix}\cos^2\theta_i & \sin\theta_i\cos\theta_i \\ \sin\theta_i\cos\theta_i & \sin^2\theta_i\end{bmatrix}\right)^{-1} \\ &= \frac{\sum_{i=2}^{n}\begin{bmatrix}\sin^2\theta_i & -\sin\theta_i\cos\theta_i \\ -\sin\theta_i\cos\theta_i & \cos^2\theta_i\end{bmatrix}}{r_c^2\sum_{i<j,i=2,j=3}^{i=n-1,j=n}\sin^2(\theta_i-\theta_j)}\end{aligned} \tag{11}$$

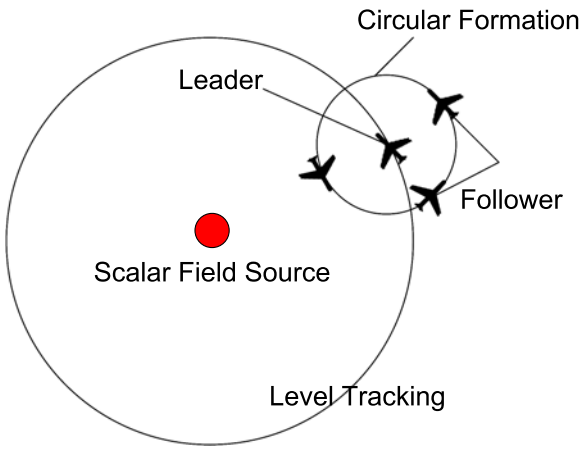

Fig. 1 Level tracking and circular formation

With Assumption 3, Substituting Eqs. 10 and 11 into Eq. 9 results in that

$$||\Delta\vec{G}|| \le \frac{r_c\delta_1}{\sum_{i<j,i=2,j=3}^{i=n-1,j=n}\sin^2(\theta_i-\theta_j)}||g(\theta_2,\theta_3,\cdots)|| \tag{12}$$

where, $g(\cdot)$ is a bounded function of clock angles.

Remark 2 It is observed from Eq. 12 that the gradient estimation error bound depends on the radius r_c of the circular formation. Smaller radius may result in a more accurate estimation. However, the formation radius is constrained by two factors. One is the UAV physical constraints such as the bounded UAV heading rate. The other factor is that if the radius is too small, then the measured field differences between UAVs are very tiny so that measurement noise may lead to large estimation error.

Remark 3 It also can be noted from Eq. 12 that the gradient estimation error bound depends on the space separation of the follower UAVs. For example, three UAVs including one leader and two followers are used for source seeking.

In this case, n=3 and the gradient estimation error bound is as follows:

$$||\Delta\vec{G}|| \le \frac{r_c\delta_1}{\sin^2(\theta_2-\theta_3)}||g(\theta_2,\theta_3)||. \tag{13}$$

$\theta_2-\theta_3=0$ implies that the two followers are located at the same point and $|\theta_2-\theta_3|=\pi$ implies that the three UAVs are collinear. Since $\sin(\theta_2-\theta_3)=0$, $(P^T P)$ is singular, which implies that there is a large estimation error. When $|\theta_2-\theta_3|=\frac{\pi}{2}$, $\sin(|\theta_2-\theta_3|)=1$ and in turn it implies that the estimation error bound attains the minimum.

3.2 Moving Source Velocity Estimate

Based on the estimated gradient, now one can proceed to estimate the moving source velocity. According to the definition of the scalar field, differentiating the scalar field at the leader location with respect to time yields that

$$\dot{f}_1 = \frac{\partial f}{\partial x_1}(\dot{x}_1 - v_{sx}) + \frac{\partial f}{\partial y_1}(\dot{y}_1 - v_{sy}). \tag{14}$$

The following adaptive observer is proposed to estimate the velocity:

$$\dot{\hat{f}}_1 = G_x(\dot{x}_1 - \hat{v}_{sx}) + G_y(\dot{y}_1 - \hat{v}_{sy}) + L\Delta f_1 + ksign(\Delta f_1). \quad (15)$$

where, L and k are the design gains, $\hat{f}_1$ is the estimated scalar field value at the leader location, $(\hat{v}_{sx}, \hat{v}_{sy})^T$ is the moving source velocity estimate and $\Delta f_1 = f_1 - \hat{f}_1$ is the field estimation error. Here, $\Delta v_{sx} = v_{sx} - \hat{v}_{sx}$, and $\Delta v_{sy} = v_{sy} - \hat{v}_{sy}$. As there exists error in the gradient estimate, the sign function is introduced to reject this error. Differentiating the scalar field estimation error Δf_1 with respect to time leads to that

$$\begin{aligned}\Delta \dot{f}_1 &= \dot{f}_1 - \dot{\hat{f}}_1 \\ &= -[G_x(\Delta v_{sx}) + G_y(\Delta v_{sy}) + \Delta G_x(\dot{x}_1 - v_{sx}) \\ &\quad + \Delta G_y(\dot{y}_1 - v_{sy})) + L\Delta f_1 + ksign(\Delta f_1)]\end{aligned} \quad (16)$$

As discussed in the previous section, the gradient estimation error is affected by the circular formation. Here, it is assumed that the gradient estimation error is bounded and small enough. Consider the following Lyapunov function candidate:

$$V_1 = \frac{1}{2}\left(\Delta f_1^2 + \Delta v_{sx}^2 + \Delta v_{sy}^2\right). \quad (17)$$

Differentiating this Lyapunov function leads to

$$\dot{V}_1 = \Delta f_1 \Delta \dot{f}_1 + \Delta v_{sx}\Delta \dot{v}_{sx} + \Delta v_{sy}\Delta \dot{v}_{sy}. \quad (18)$$

Substituting Eq. 16 into Eq. 18 yields that

$$\begin{aligned}\dot{V}_1 = &-\Delta f_1[G_x(\Delta v_{sx}) + G_y(\Delta v_{sy}) + \Delta G_x(\dot{x}_1 - v_{sx}) \\ &+ \Delta G_y(\dot{y}_1 - v_{sy})) + L\Delta f_1 + ksign(\Delta f_1)] \\ &+ \Delta v_{sx}\Delta \dot{v}_{sx} + \Delta v_{sy}\Delta \dot{v}_{sy}.\end{aligned} \quad (19)$$

The adaptive update laws for $\hat{v}_{sx}$ and $\hat{v}_{sy}$ are as follows:

$$\dot{\hat{v}}_{sx} = -\Delta f_1 G_x;\ \dot{\hat{v}}_{sy} = -\Delta f_1 G_y. \quad (20)$$

The gain k is designed as follows:

$$\begin{aligned}k &= ||\Delta G_x(\dot{x}_1 - v_{sx}) + \Delta G_y(\dot{y}_1 - v_{sy})||_\infty \\ &\le ||\Delta \vec{G}||_\infty (v_1 + ||\vec{v}_s||).\end{aligned} \quad (21)$$

where, v_1 is the airspeed of the leader UAV and $||\vec{v}_s||$ is the speed of the moving source.

Substituting Eqs. 20 and 21 into Eq. 19 results in that

$$\begin{aligned}\dot{V}_1 &= -L\Delta f_1^2 - k|\Delta f_1| \\ &\quad -\Delta f_1(\Delta G_x(\dot{x}_1 - v_{sx}) + \Delta G_y(\dot{y}_1 - v_{sy})) \\ &\le -L\Delta f_1^2\end{aligned} \quad (22)$$

It is noted from Eq. 22 that, Δf_1, Δv_{sx} and Δv_{sy} are bounded. In addition, according to Assumption 3, $\Delta \dot{\vec{G}} = \dot{\vec{G}} - \nabla \dot{f}$ and $\Delta \dot{f}_1$ are also bounded, which implies that $\ddot{V}_1$ is bounded. Therefore, according to Barbalat's lemma, $\dot{V}_1 = 0$ as $t \to \infty$, which in turn implies that $\Delta f_1 = 0$ and $\Delta \dot{f}_1 = 0$ as $t \to \infty$. Hence, one can obtain the following equation from Eq. 16:

$$-G_x(\Delta v_{sx}) - G_y(\Delta v_{sy}) = (\dot{x}_1 - v_{sx}, \dot{y}_1 - v_{sy})\Delta \vec{G} + ksign(\Delta f_1) \quad (23)$$

$$||G_x(\Delta v_{sx}) + G_y(\Delta v_{sy})|| \le 2||\Delta \vec{G}||_\infty (v_1 + ||\vec{v}_s||) \quad (24)$$

$$||\vec{G}||||(\Delta v_{sx}, \Delta v_{sy})|| \cos\Phi \le 2||\Delta \vec{G}||_\infty (v_1 + ||\vec{v}_s||) \quad (25)$$

It can be known from Eq. 20 that when $\Delta f_1 \to 0$, $(\Delta v_{sx}, \Delta v_{sy})$ will be constant. Then, Φ is dependent on $\vec{G}$. For any $\Phi \in [-\pi, \pi)$, the Eq. 25 holds. Thus, it can be derived that

$$||\Delta \vec{v}_s|| = ||(\Delta v_{sx}, \Delta v_{sy})|| \le \frac{2||\Delta \vec{G}||_\infty (v_1 + ||\vec{v}_s||)}{\min_{(x,y)\in S} ||\vec{G}||}. \quad (26)$$

where, S denotes the area in which the leader UAV locates. It can be observed from Eq. 26 that, the source velocity estimation error depends on the minimum gradient. When the UAV flies close to the source, the gradient will increase so that the

velocity estimation error will be reduced. It can also be concluded that the moving source velocity estimation error is determined by the gradient error. Therefore, if the gradient error is small enough, then one can obtain an accurate estimate for the source velocity.

4 Level Tracking of Multiple UAVS

In the previous section, scalar field gradient and moving source velocity are estimated and the estimation errors are also analyzed. Now it is ready to design controllers for UAVs so that level tracking around the source is achieved. In this section, a guidance law based on the estimated gradient and moving source velocity is proposed for the leader UAV. Heading rate controller for the leader UAV is designed such that the desired heading generated by the guidance law is always followed. The overall control structure is described in Fig. 2. Then, level tracking error is explored in terms of the gradient estimation error. Lastly, in order for follower UAVs to achieve circular formation, heading rate controllers are designed.

4.1 Guidance Law and Heading Rate Controller Design for Leader UAV

Level tracking of the scalar field by the leader UAV will be discussed in sequel. Different from our previous work [25], moving source is considered in this paper. Thus, the guidance law proposed in [25] needs to be modified. Firstly, consider the leader UAV kinematics [17]:

$$\dot{x}_1 = v_1 \cos\psi_1 = v_{1r}\cos\chi_1 + \hat{v}_{sx}$$
$$\dot{y}_1 = v_1 \sin\psi_1 = v_{1r}\cos\chi_1 + \hat{v}_{sy}$$
$$\dot{\psi}_1 = w_1 = \frac{\dot{\chi}_1}{\gamma(\psi_1)}, \tag{27}$$

where, χ_1 denotes the course angle, v_{1r} denotes the relative speed, and

$$v_{1r} = (v_1^2 + \hat{v}_{sx}^2 + \hat{v}_{sy}^2 - 2v_1(\hat{v}_{sx}\cos\psi_1 + \hat{v}_{sy}\sin\psi_1))^{\frac{1}{2}}, \tag{28}$$

$$\chi_1 = \arctan 2(v_1\sin\psi_1 - \hat{v}_{sy}, v_1\cos\psi_1 - \hat{v}_{sx}), \tag{29}$$

$$\gamma(\psi_1) = \frac{v_1^2 - v_1(\hat{v}_{sx}\cos\psi_1 + \hat{v}_{sy}\sin\psi_1)}{v_{1r}^2}. \tag{30}$$

Remark 4 In Assumption 2, the source velocity $v_s < v_l$. In order for the leader UAV to achieve level tracking, the leader velocity should satisfy the following condition: $v_1 \geq v_l$. It is also assumed that the prespecified field level value is f_d, and the following guidance law for the relative course angle is proposed.

$$\chi_1^d = \arctan 2(G_y, G_x) - \pi + 2\arctan\left(\frac{f_d}{f_1}\right) \in [-\pi, \pi) \tag{31}$$

Based on this desired course angle, we can also compute the desired heading angle by using Eq. 29. According to the results in [17] and [25], if there exist no errors in gradient estimate and moving source estimate, the proposed guidance law can drive the leader UAV to the desired level set. However, estimation errors are usually inevitable in practice. Therefore, next, it proceeds to analyze the stability and level tracking error bound. Here, it is assumed that the UAV heading angle is always equal to the desired one. Consider the following function:

$$V_2 = \frac{1}{2}(f_1 - f_d)^2. \tag{32}$$

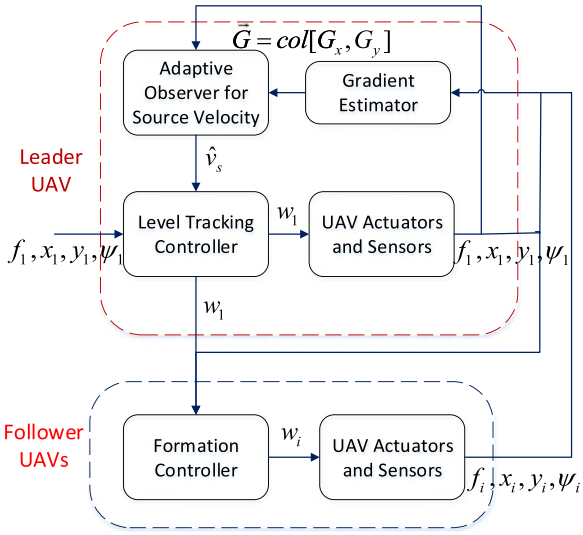

Fig. 2 Control structure for source seeking

Differentiating this function (32) with respect to time leads to that (see Eq. 33).

$$
\begin{aligned}
\dot{V}_2 &= (f_1 - f_d)\,\dot{f}_1 \\
&= (f_1 - f_d)\left[\frac{\partial f}{\partial x_1}, \frac{\partial f}{\partial y_1}\right]\left[\dot{x}_1 - v_{sx}, \dot{y}_1 - v_{sy}\right]^T \\
&= -(f_1 - f_d)\left[\frac{\partial f}{\partial x_1}, \frac{\partial f}{\partial y_1}\right]\left[v_{1r}\cos\left(\chi_1^d\right) + \hat{v}_{sx} - v_{sx}, v_{1r}\sin\left(\chi_1^d\right) + \hat{v}_{sy} - v_{sy}\right]^T \\
&= -(f_1 - f_d)\left[\frac{\partial f}{\partial x_1}, \frac{\partial f}{\partial y_1}\right]\left[v_{1r}\frac{G_x(f_1^2 - f_d^2) - 2G_y f_1 f_d}{\sqrt{G_x^2 + G_y^2}(f_1^2 + f_d^2)} - \Delta v_{sx}, v_{1r}\frac{G_y(f_1^2 - f_d^2) + 2G_x f_1 f_d}{\sqrt{G_x^2 + G_y^2}(f_1^2 + f_d^2)} - \Delta v_{sy}\right]^T \\
&= -(f_1 - f_d)\left[v_{1r}\frac{\left(\frac{\partial f}{\partial x_1}^2 + \frac{\partial f}{\partial y_1}^2 + \frac{\partial f}{\partial x_1}\Delta G_x + \frac{\partial f}{\partial y_1}\Delta G_y\right)\left(f_1^2 - f_d^2\right) - 2\left(\frac{\partial f}{\partial x_1}\Delta G_y - \frac{\partial f}{\partial y_1}\Delta G_x\right) f_1 f_d}{\sqrt{G_x^2 + G_y^2}\left(f_1^2 + f_d^2\right)}\right. \\
&\qquad \left. - \frac{\partial f}{\partial x_1}\Delta v_{sx} - \frac{\partial f}{\partial y_1}\Delta v_{sy}\right] \\
&\le -v_{1r}(f_1 + f_d)\frac{||\nabla f||^2(f_1 - f_d)^2}{\sqrt{G_x^2 + G_y^2}(f_1^2 + f_d^2)} + v_{1r}\frac{(|f_1^2 - f_d^2||f_1 - f_d| + 2|f_1 - f_d|f_1 f_d)||\Delta G||||\nabla f||}{\sqrt{G_x^2 + G_y^2}(f_1^2 + f_d^2)} \\
&\quad + ||\nabla f||||\Delta v_s||f_1 - f_d| \qquad (33)
\end{aligned}
$$

It can be observed from Eq. 33 that if

$$
|f_1 - f_d| > \frac{(|f_1^2 - f_d^2| + 2f_1 f_d)||\Delta G||}{||\nabla f||(f_1 + f_d)} + \frac{||\Delta v_s||\sqrt{G_x^2 + G_y^2}(f_1^2 + f_d^2)}{v_{1r}||\nabla f||(f_1 + f_d)},
$$

then, it can be obtained that

$$
\dot{V}_2 < 0 \qquad (34)
$$

It can be concluded that the level tracking error $|f_1 - f_d|$ is bounded and eventually converges to the following region: $[0, \frac{v_{1r}(|f_1^2 - f_d^2| + 2f_1 f_d)||\Delta G|| + ||\Delta v_s||\sqrt{G_x^2 + G_y^2}(f_1^2 + f_d^2)}{v_{1r}||\nabla f||(f_1 + f_d)}]$.

Next, the heading rate controller is designed so that the UAV always follows the desired heading angle. Here, we firstly design a sliding mode based course rate controller as follows:

$$
\dot{\chi}_1 = -w_1^0 sign(\chi_1 - \chi_1^d), \qquad (35)
$$

where w_1^0 is a positive constant.

To guarantee that the UAV can follow the desired course, it is assumed that $|\dot{\chi}_1^d| < w_1^0$. Let $V_3 = (\chi_1 - \chi_1^d)^2$, and then the time derivative

$$
\begin{aligned}
\dot{V}_3 &= 2\left(\chi_1 - \chi_1^d\right)\left(-w_1^0 sign\left(\chi_1 - \chi_1^d\right) - \dot{\chi}_1^d\right) \\
&= -2k\left(\chi_1 - \chi_1^d\right)^2 \le 0, \qquad (36)
\end{aligned}
$$

where $k > 0$ and $-w_1^0 sign(\chi_1 - \chi_1^d) = -k(\chi_1 - \chi_1^d) + \dot{\chi}_1^d$.

Based on this course rate, the heading rate controller can also be obtained by using Eq. 30. Using the proposed course rate controller (35), the actual course of the leader UAV will eventually converge to the desired one. Hence, the

leader UAV will finally fly along the desired level curve around the source, if the estimated gradient and moving source velocity is accurate enough. It is worth noting that, the course rate control parameter w_1^0 and the constant airspeed u_1 of the leader must be carefully selected so that the follower UAVs have a high enough level of maneuverability to follow the leader. Since the sliding mode controller may lead to undesirable chattering, in order to overcome this problem, the following continuous function is used to replace the sliding mode controller (35):

$$\dot{\chi}_1 = -w_1^0 sat(\mu(\chi_1 - \chi^d)), \tag{37}$$

where $\mu > 0$ and $sat(x) = \begin{cases} 1, \text{ if } x > 1 \\ x, \text{ if } |x| \leq 1 \\ -1, \text{ if } x < -1 \end{cases}$.

4.2 Heading Rate Controller Design for Follower UAVs

The proposed course rate controller for the leader can also be transformed to the heading rate controller. In this section, follower heading rate controller are designed so that the circular formation can be achieved and well maintained. It is ready to proceed to design the heading rate controller for the follower UAVs. The heading rate design procedure has been presented in our previous work [25]. Therefore, in this paper, only sketched steps are provided.

The relative position of the follower UAV with respect to the leader can be represented as

$$x_{i1} = x_i - x_1, y_{i1} = y_i - y_1, i = 2, 3, \cdots n. \tag{38}$$

χ_i is introduced to denote the relative heading angle of the follower UAV with respect to the leader. Then, relative kinematics can be represented as

$$\begin{cases} \dot{x}_{i1} = v_{i1} \cos \chi_i \\ \dot{y}_{i1} = v_{i1} \sin \chi_i \end{cases} i = 2, 3, \cdots n. \tag{39}$$

where, $v_{i1} = ((\dot{x}_i - \dot{x}_1)^2 + (\dot{y}_i - \dot{y}_1)^2)^{\frac{1}{2}}$ and $\chi_i = \arctan 2(\dot{y}_i - \dot{y}_1, \dot{x}_i - \dot{x}_1)$. Here, it can be observed that if $v_i > v_1$, $v_{i1} \geq \Delta > 0$. In this paper, it is assumed that $v_i > v_1$ and the airspeeds of all followers are the same.

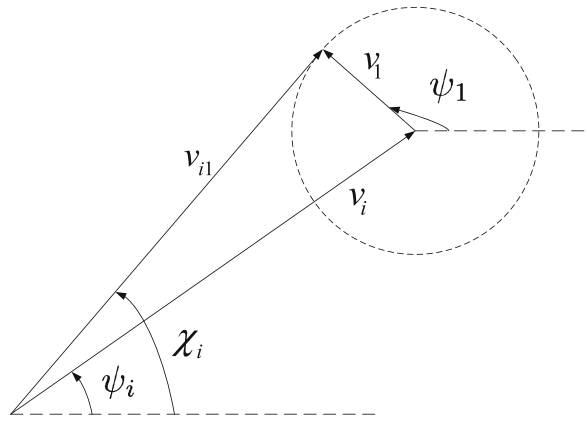

Fig. 3 Relative heading and actual heading

The relationship between the actual heading rate and the relative heading rate can be represented by the following formula

$$\dot{\psi}_i = \frac{[v_{i1}\dot{\chi}_i + w_1 v_1 \cos(\chi_i - \psi_1)]}{v_i \cos(\chi_i - \psi_i)}. \tag{40}$$

It can be observed from Fig. 3 that, if $v_i > v_1$, $\cos(\chi_i - \psi_i) > 0$. Furthermore, if $\dot{\chi}_i$ is bounded, $\dot{\psi}_i$ can also be bounded according to the Eq. 40.

Next, it proceeds to design the heading rate controller for each follower UAV to achieve a circular formation subject to the physical constraints of the fixed wing UAV. The leader UAV is located at the center of the formation and executes

Table 1 specifications of the UAV and control law parameters

Parameter	Value
Leader airspeed u_1	8 m/s
Follower airspeed u_i	20 m/s
w_1^0	0.1 rad/s
$w_{\max}$	0.5 rad/s
$f_{\max}$	800
f_d	600
α	1/1600
β	1
μ	50
$\delta\omega$	5
k_1	5
v_{sx}	2 m/s
v_{sy}	4 m/s
k	0.4

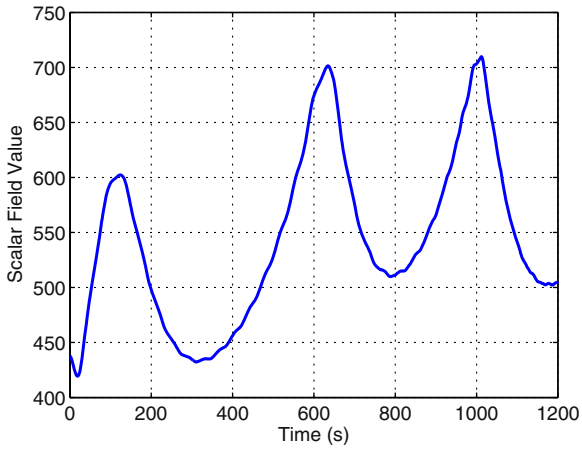

Fig. 4 Scalar field level tracking (scenario one)

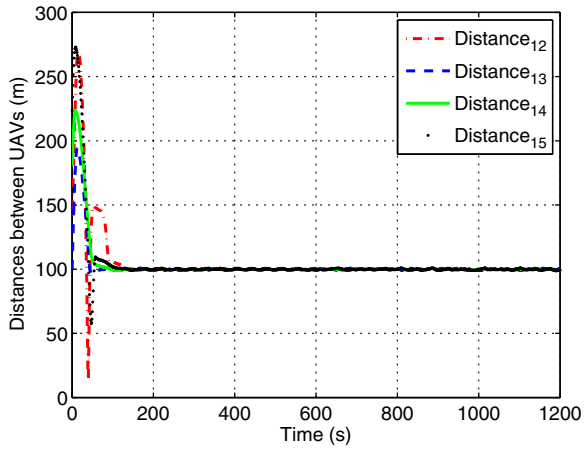

Fig. 6 Distances between leader UAV and four follower UAVs (scenario one)

the mission of level tracking. The follower UAVs are located along the circle around the leader and keep a desired distance r_c to the leader (see Fig. 1).

The relative heading rate is designed as follows

$$\dot{\chi}_i = \frac{1}{r_c}[v_{i1} + \delta w \tanh(k_1(x_{i1}\cos\chi_i + y_{i1}\sin\chi_i))], \tag{41}$$

where $\delta w > 0$ and $k_1 > 0$.

Based on the designed relative heading rate (41), the heading rate control input can be obtained by Eq. 40. According to the result in [25], the follower can finally converge to the desired circular orbit around the leader.

5 Simulation Results

In this section, three simulation scenarios using the proposed approach will be presented. In the first scenario, five UAVs including one leader and four followers are controlled to execute the mission of source seeking while the moving source velocity is not estimated, where the radius of the circular formation is 100 m. In the second scenario, as compared to the first scenario, the moving source velocity is estimated and applied to the controller. In the third scenario, the radius of the circular formation are smaller than those in the first two scenarios. Here, the scalar field $f(\vec{r}) = f_{\max}[1 - \tanh(\alpha||\vec{r} - \vec{r}_s||^{\beta})]$, $\alpha > 0, \beta > 0$ is

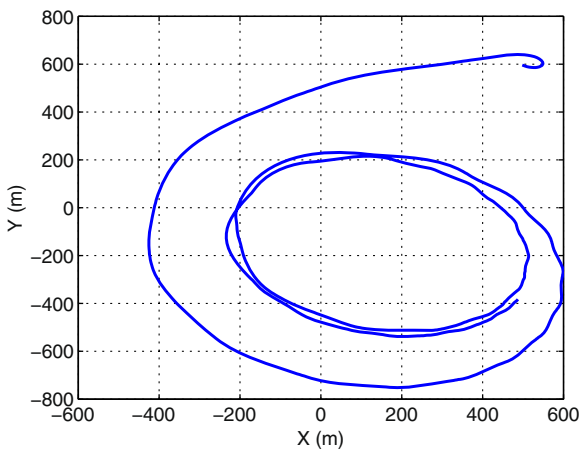

Fig. 5 Trajectory of the leader UAV (scenario one)

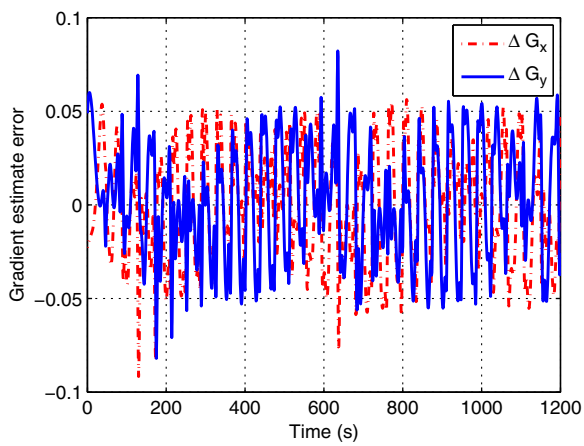

Fig. 7 Gradient estimation error (scenario two)

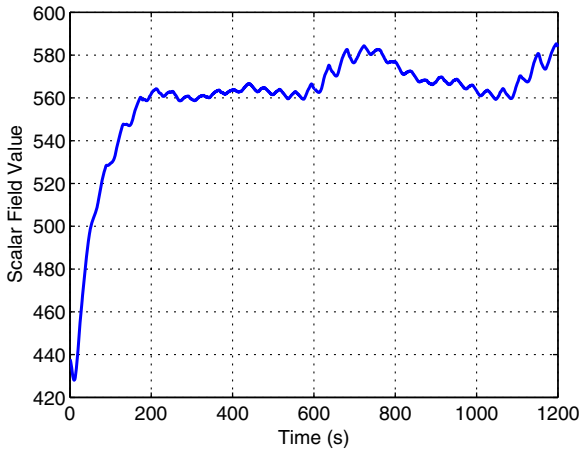

Fig. 8 Scalar field level tracking (scenario two)

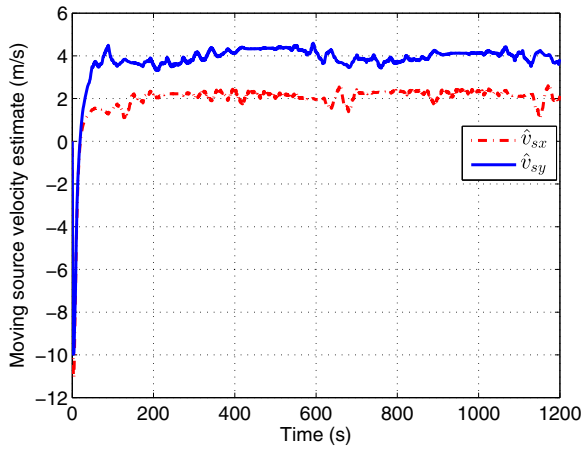

Fig. 10 Moving source velocity estimation (scenario two)

used. It is assumed that the initial position of the source is $\vec{r}_s(0) = (0, 0)^T$. Table 1 shows the specifications of the UAV, the scalar field parameters and the control law parameters.

In scenario one, the initial positions of the five UAVs are as follows: (500,600), (600,700), (600,600), (650,500) and (700,500). It can be observed from Fig. 4 that, the level tracking error is very large due to the source movement. Figure 5 shows the trajectory of the leader UAV, where it can be seen that, the distance between the UAV and the source significantly changes, which may result in the loss of source. Figure 6 shows the distances between the leader UAV and the four follower UAVs. As claimed in the section IV, the follower UAVs converge to the circular orbit with a desired distance to the leader UAV.

In scenario two, the initial positions of the five UAVs are the same as those in scenario one. Compared with scenario one, scenario two takes the moving source velocity into account. An adaptive observer is utilized to estimate the velocity which is used to generate the guidance law for the leader UAV. Figure 7 shows the gradient estimate error. Since UAVs are not evenly distributed along the circular orbit, there always exists gradient estimate error. Figures 8 and 9 depict the

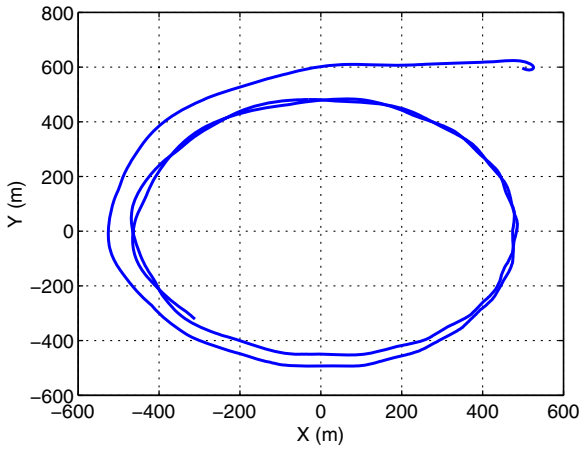

Fig. 9 Leader UAV trajectory w.r.t. source (scenario two)

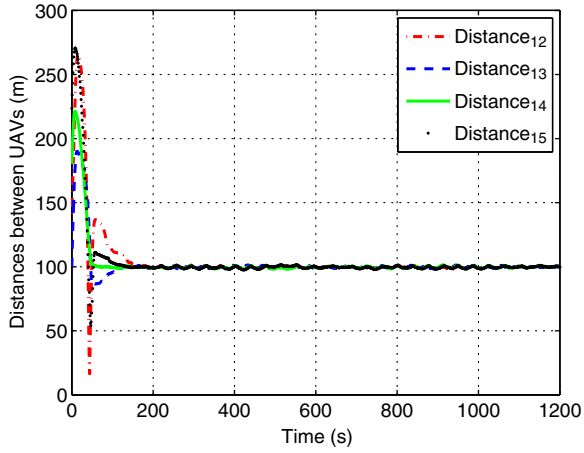

Fig. 11 Distances between UAVs (scenario two)

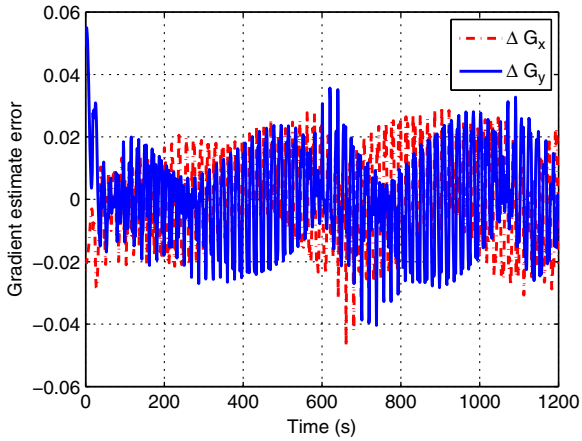

Fig. 12 Gradient estimation error (scenario three)

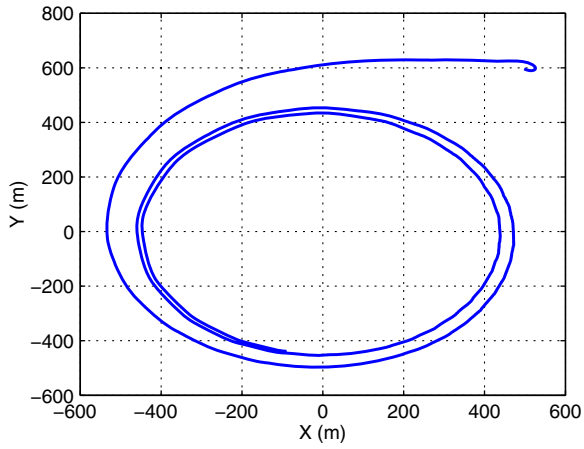

Fig. 14 Leader UAV trajectory w.r.t. source (scenario three)

measured scalar field at the leader location and the leader UAV trajectory with respect to the moving source, respectively. Figure 10 shows the moving source velocity estimation, where the estimate converges to the vicinity of the actual value. Due to the existence of gradient estimation error, the velocity estimation error can not converge to zero. Figure 11 describes the distances between leader and follower UAVs. Compared with the scenario one, it is observed from Fig. 8 that the level tracking error is much smaller in scenario two, which verifies the effectiveness of the proposed adaptive observer and controllers.

In the last scenario, the desired formation radius is smaller than those in the previous two scenarios, where the radius is 50 m. It is seen from Fig. 12 that, the gradient estimation error is smaller than that in scenario two, which implies that the gradient estimation accuracy depends on the formation radius. Figures 13, 14 and 15 show the scalar field measurement, UAV trajectory and moving source estimation, respectively. It can be concluded that the smaller gradient estimation error results in better level tracking performance.

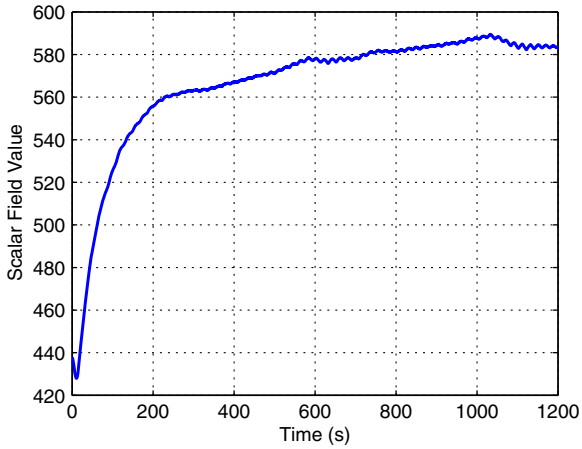

Fig. 13 Scalar field level tracking (scenario three)

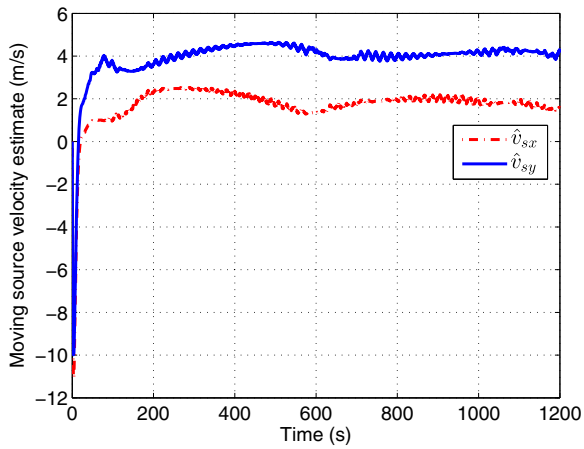

Fig. 15 Moving source velocity estimation (scenario three)

6 Conclusions

Cooperation of multiple UAVs for moving source seeking is discussed in this paper. Scalar field gradient is estimated by using a least-squares method. Based on the gradient estimate, an adaptive observer is proposed to estimate the moving source velocity. Then, both gradient and moving source velocity estimates are used to generate a guidance law for the leader UAV to achieve level tracking. Heading rate controllers are designed for UAVs so that level tracking and circular formation are executed. Furthermore, gradient estimate error and its influence on moving source velocity estimation and level tracking accuracy are also analyzed.

References

1. Cochran, J., Krstic, M.: Nonholonomic source seeking with tuning of angular velocity. IEEE Trans. Autom. Control **54**, 717–731 (2009)
2. Zhang, C., Arnold, D., Ghods, N., Siranosian, A., Krstic, M.: Source seeking with nonholonomic unicycle without position measurement and with tuning of forward velocity. Syst. Control Lett. **56**, 245–252 (2007)
3. Matveev, A.S., Teimoori, H., Savkin, A.V.: Navigation of a unicycle-like mobile robot for environmental extremum seeking. Automatica **47**(1), 85–91 (2011)
4. Ogren, P., Fiorelli, E., Leonard, N.E.: Cooperative control of mobile sensor networks: adaptive gradient climbing in a distributed environment. IEEE Trans. Autom. Control **49**(8), 1292–1302 (2004)
5. Han, J., Xu, Y., Di, L., Chen, Y.: Low-cost multi-UAV technologies for contour mapping of nuclear radiation field. J. Intell. Robot. Syst. **70**(1–4), 401–410 (2013)
6. Han, J., Chen, Y.: Cooperative source seeking and contour mapping of a diffusive signal field by formations of multiple UAVs. IEEE International Conference on Unmanned Aircraft Systems (ICUAS), pp. 35–40, Atlanta (2013)
7. Azuma, S., Sakar, M.S., Pappas, G.J.: Stochastic source seeking by mobile robots. IEEE Trans. Autom. Control **57**(9), 2308–2321 (2012)
8. Zhang, F., Leonard, N.E.: Cooperative filters and control for cooperative exploration. IEEE Trans. Autom. Control **55**(3), 650–663 (2010)
9. Hu, J., Hu, X.: Nonlinear filtering in target tracking using cooperative mobile sensors. Automatica **46**(12), 2041–2046 (2010)
10. Biyik, E., Arcak, M.: Gradient climbing in formation via extremum seeking and passivity-based coordination rules. In: 46th IEEE Conference on Decision and Control, pp. 3133–3138, New Orleans, LA (2007)
11. Ghods, N., Krstic, M.: Multiagent deployment over a source. IEEE Trans. Control Syst. Technol. **20**(1), 277–285 (2012)
12. Li, S., Guo, Y.: Distributed source seeking by cooperative robots: all-to-all and limited communications. IEEE International Conference on Robotics and Automation, pp. 1107–1112. USA (2012)
13. Brinon-Arranz, L., Seuret, A., Canudas-de-Wit, C.: Collaborative estimation of gradient direction by a formation of AUVs under communication constraints. In: 50th IEEE Conference of Decision and Control and European Control Conference (CDC-ECC), pp. 5583–5588 (2011)
14. Moore, B.J., Canudas-de-Wit, C.: Source seeking via collaborative measurements by a circular formation of agents. In: American Control Conference (ACC), pp. 6417–6422 (2010)
15. Frew, E., Lawrence, D.: Cooperative standoff tracking of moving targets using Lyapunov guidance vector fields. AIAA J. Guid. Control. Dyn. **31**(2), 290–306 (2008)
16. Summers, T.H., Akella, M.R., Mears, M.J.: Coordinated standoff tracking of moving targets: control laws and information architectures. AIAA J. Guid. Control. Dyn. **32**(1), 56–69 (2009)
17. Zhu, S., Wang, D., Low, C.B.: Ground target tracking using UAV with input constraints. J. Intell. Robot. Syst. **69**(1–4), 417–429 (2013)
18. Zhu, S., Wang, D.: Adversarial ground target tracking using UAVs with input constraints. J. Intell. Robot. Syst. **65**(1–4), 521–532 (2012)
19. Paley, D.A., Peterson, C.: Stabilization of collective motion in a time-invariant flowfield. AIAA J. Guid. Control. Dyn. **32**(3), 771–779 (2009)
20. Peterson, C., Paley, D.A.: Cooperative control of unmanned vehicle in a time-varying flowfield. In: Proceedings of AIAA Guidance, Navigation, and Control Conference (2009)
21. Peterson, C., Paley, D.A.: Multiple coordination in an estimated time-varying flowfield. AIAA J. Guid. Control. Dyn. **34**(1), 177–191 (2011)
22. Xu, B., Gao, D., Wang, S.: Adaptive neural control based on HGO for hypersonic flight vehicles. Sci. China Inf. Sci. **54**(3), 511–520 (2011)
23. Xu, B., Sun, F., Yang, C., Gao, D., Ren, J.: Adaptive discrete-time controller design with neural network for hypersonic flight vehicle via back-stepping. Int. J. Control. **84**(9), 1543–1552 (2011)
24. Xu, B., Sun, F., Liu, H., Ren, J.: Adaptive kriging controller design for hypersonic flight vehicle via back-stepping. IET Control Theory Appl. **6**(4), 487–497 (2012)
25. Zhu, S., Wang, D., Low, C.B.: Cooperative control of multiple UAVs for source seeking. J. Intell. Robot. Syst. **70**(1–4), 293–301 (2013)